Chapter 5

Mesospheric Temperature Variations During SSW Events

5.1 Background

The results discussed in earlier Chapters were mainly obtained from the ground-based observations which were related to the understanding of large- and short-timescale variations in the mesosphere, solar effects in the mesosphere, statistical characterization of gravity wave parameters, and vertical coupling of the atmospheres under varying atmospheric conditions.

In this Chapter, the focus is to understand the global nature of mesospheric temperature variability during SSW events. The phenomenon of sudden stratospheric warming (SSW) has been introduced in Chapter 1 wherein, we have briefly discussed its causative mechanism, and some of the effects in the MLT region. As briefed in Chapter 1, even though SSW is a northern hemisphere high-latitude phenomena, various altitudinal and latitudinal regions of the Earth's atmosphere can be affected during SSW events. In addition to NIRIS observations, the results presented in this Chapter are based on the data obtained from multiple satellite-based observations, and MERRA data sets. The results obtained on the nature of latitudinal variation of mesospheric tempera-

tures during SSW events which are based on 11 SSW evets that occurred during 2004 to 2013 will be discussed. It has been found that during SSW events the well-known mesospheric cooling over the northern hemispheric high-latitudes turns to heating over mid-latitudes and then reverts to cooling closer to equatorial regions. This trend continues into the southern hemisphere as well. These variations in the mesospheric temperatures at different latitudes have been characterized based on northern hemispheric stratospheric temperature enhancements at high-latitudes during SSW periods. Such a characterization in mesospheric temperatures with respect to latitudes reveals an hitherto unknown intriguing nature of the latitudinal coupling in the mesosphere that gets set up during the SSW events.

5.2 Introduction

As discussed in Chapter 1, SSW is a large-scale phenomenon that occurs mostly in the northern hemispheric polar stratosphere during winter time, and is characterized by a drastic rise in temperature within a few days. An SSW event is called 'minor' if the mean temperature at or below the 10 hPa pressure level (∼32 km) poleward of 60^o rises by at least 25 K within a period of a week. An event is considered as 'major' if, in addition to increased temperature, zonal mean eastward winds reverse at these altitude and latitude region [*McInturff* (1978); *Labitzke* (1981)]. SSW is attributed to the interaction of zonal winds with vertically propagating planetary waves (PWs) forced from the troposphere and their effect in terms of quasi-16-day waves have also been seen to be present over low- and equatorial-latitude E- and F-regions of the ionosphere [e.g., *Laskar et al.* (2014)].

It has also been shown that the westward acceleration of zonal winds over northern hemispheric high-latitudes occurs during SSW periods in the presence of PWs [*Matsuno* (1971)]. Further, it has been shown that during SSW events mesospheric cooling occurs at high-latitudes [*Labitzke* (1972), *Labitzke* (1981)],

which has also been confirmed by the OH airglow temperature measurements over both northern and southern hemispheres (NH & SH) [e.g., *Walterscheid et al.* (2000); *Azeem et al.* (2005)]. In the NH observation from Eureka, Canada (80^{o}N, 86^{o}W) mesospheric cooling of ∼25 K was observed during 13 to 14 February 1993 [*Walterscheid et al.* (2000)] while, measurements over South Pole station in Antarctica showed a decrease in mesospheric temperatures of ∼ 15 K prior to the stratospheric warmings of May 1995 and July 2002 [*Azeem et al.* (2005)].

Moreover, by comparison of SABER temperatures at different pressure levels it was noted that while the stratospheric temperature at 10 hPa pressure level increased over several days, the mesospheric temperature (in the 0.3 to 0.01 hPa pressure range) decreased simultaneously during 2002 SSW period over SH at 80^{o}S latitude [*Siskind et al.* (2005)]. Further, a new meridional circulation has been found to get set in the MLT region during SSW events owing to the concomitant increase in the lower thermospheric temperatures in the altitudes above cooler mesopause in high-latitudes [*Laskar and Pallamraju* (2014)]. Thus, it is imperative that a comprehensive investigation on latitudinal distribution of mesospheric temperatures be carried out, especially during SSW events.

Greater information on mesospheric temperatures and winds are available at high-latitudes compared with those at equatorial-, low- and mid-latitudes for the periods during SSW events. Lower mesospheric temperatures at equatorial-latitudes were first obtained using rocket-sondes from Thumba (8.5^{o}N, 76^{o}E), in India, wherein it was reported that occasional warmings occur in the upper stratosphere and lower mesosphere during SSW periods [*Mukherjee and Ramanamurty* (1972)]. Recently, for 2009 SSW event using Rayleigh lidar observations a warm mesospheric condition has been reported [*Sridharan et al.* (2010)] over Gadanki (13.5^{o}N, 79.2^{o}E), a low-latitude location in India. These observations were also found to be consistent with the SABER derived temperatures obtained over the same location. In all these studies the temperature

behaviour at altitudes below 80 km was investigated. Due to the paucity of continuous ground-based measurements of mesospheric temperatures over equatorial- to mid-latitudes, the behaviour of the mesosphere during SSW periods at these latitudes is not well-understood.

In this study, we have used high cadence NIRIS derived mesospheric temperatures from a low-latitude location (Gurushikhar), satellite derived global distribution of mesospheric temperatures from SABER, OSIRIS, and SOFIE, and stratospheric temperatures and zonal winds as derived from Modern Era Retrospective-analysis for Research and Applications (MERRA) datasets to characterize the behaviour of mesospheric temperatures along the North-South meridian in both the hemispheres. Stratospheric temperatures and winds at high-latitudes ($>60^o$N) are considered as tracers of the stratospheric behaviour in the NH and hence the occurrence of SSW events. In that regard the observed stratospheric temperature enhancements and zonal wind reversals at NH high-latitudes during SSW periods would indicate the prevalent planetary wave activity.

5.3 Measurement Techniques

The results discussed in this Chapter are based on the NIRIS data, observations from multi-satellite platforms, and reanalysis data. The details of these data sets have been discussed in Chapter 2 and hence, are only listed below:

1. NIRIS derived mesospheric temperatures have been obtained from O_2(0-1) atmospheric and OH(6-2) vibrational band spectra which correspond to altitude regions of 94 and 87 km, respectively. These observations have been carried out from PRL's optical aeronomy observatory at Gurushikhar, Mount Abu (24.6^oN, 72.8^oE) during January 2013. For the study reported in this Chapter zenith temperature measurements are used.

2. MERRA data have been used to obtain the stratospheric temperatures poleward of 60^{o}N and longitudinally averaged zonal wind at 60^{o}N at 10 hPa pressure level (∼32 km).

3. SABER derived mesospheric temperatures for different latitudes obtained for 11 SSW events have been used. The SABER data products are briefed in Chapter 2. The estimated uncertainty in the SABER temperatures in the altitude range of 80-100 km is ±4 K [*Mertens et al.* (2001)].

4. OSIRIS derived mesospheric temperatures during 2009 and 2010 major SSW events have been used.

5. SOFIE derived (level 2A) mesospheric temperatures in the polar latitudes (65^o-85^{o}S/65^o-85^{o}N) have been used.

5.4 Observations

In this section, it is described that how the observed features in the NIRIS derived temperatures in January 2013 provided motivation for a wider investigation to understand the behaviour of global large-scale mesospheric temperature distribution that exists during SSW events. In this study, SSW temperatures and winds at 10 hPa pressure level from MERRA and SABER derived mesospheric temperatures during eleven SSW events that occurred during the past ten years (2004-2013) in the months of January and February have been used. Of these eleven SSW events, six were major and five were minor in nature.

5.4.1 NIRIS Temperatures for January 2013

The mesospheric nocturnal temperatures derived from O_2 and OH using NIRIS in the month of January 2013 during day of the year (DOY) 7-21 are shown in Figures 5.1a and 5.1b, respectively. From Figure 5.1a it may be noted that

the mesospheric temperatures at 94 km show higher values for DOY 7, 8, 16, 18, and 19 before midnight and gradually reduce later.

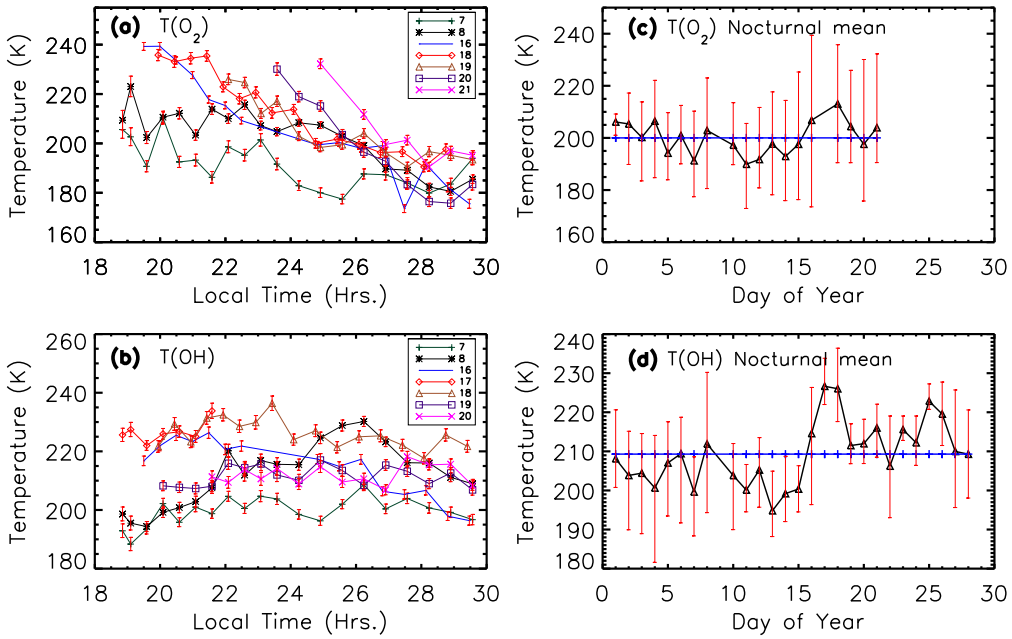

Figure 5.1: (a) NIRIS derived O_2 rotational temperatures (at 94 km) over Gurushikhar, Mount Abu for a few selected nights during SSW period are shown along with the estimated uncertainty ($\sim\pm$3K) at each of the datum points. (b) Similar plot as in Figure 5.1a but for OH temperature (at 87 km). (c) Nocturnal mean mesospheric temperatures derived from O_2(0-1) atmospheric band for the month of January 2013 (black line) and monthly mean (blue line) are shown. The red vertical bar shows the range of the derived temperatures for a given night. (d) Similar plot as in Figure 5.1c but for OH derived temperatures. It may be noted that mesospheric temperatures are elevated throughout the night (as shown in the range of temperatures) during the SSW period.

From Figure 5.1b it can be seen that on 8 January 2013 the mesospheric temperature enhancement is in the post-midnight period. On 16 January 2013 OH temperature enhancements are seen during pre-midnight hours and seem to be reduced during post-midnight. All these observations show modulations due to the presence of gravity, tidal, and planetary waves in the mesospheric temperatures at these altitudes. On 17 and 18 January the OH mesospheric temperatures are elevated for the duration of the data available in comparison with the nocturnal mean temperature value for this month (discussed below).

The dissimilar behaviour in the temperatures at these two altitudes is a result of vertically propagating gravity waves as discussed in Chapter 4. The effects of PW type scale sizes on these altitudes are discussed here using these temperature values, while the characterization of temperatures at these two altitudes in the time scales of gravity and tidal wave regimes was discussed in Chapter 3.

Figures 5.1c and 5.1d show nocturnal mean O_2 and OH rotational temperatures during January 1-21 and January 1-29, respectively, together with the range of the temperature on a given night. From these figures it can be seen that mesospheric temperatures are elevated for several nights when compared with the monthly mean values. Especially, the nightly average together with the nightly range in the O_2 and OH temperatures are enhanced during January 16 to 19 and January 16 to 26, respectively, when compared with the monthly mean. This indicates to a significant additional source of energy to the low- and mid-latitudes spanning several days.

Interestingly, the enhancement in the mesospheric temperatures as seen from NIRIS data described here were found to be occurring during a major SSW event (January 7–27, 2013; Figure 5.2h) which occurs at polar latitudes. In this context, it is relevant to note that OH band emissions from higher vibrational levels peak at higher altitudes [*Savigny et al.* (2012)]. Using SCIAMACHY (SCanning Imaging Absorption spectroMeter for Atmospheric CartograpHY on Envisat) data it was shown that the OH (6-2) emission rate profile is typically vertically shifted upwards by 1-2 km relative to the OH (3-1) band, and the OH (8-3) band is generally found to peak about 1 km higher than the OH (6-2) band [*Savigny et al.* (2012)]. The O_2(0-1) emission layer is considered to be located at 94 km altitude [*Murtagh et al.* (1990)] and the altitude of peak OH emission can be considered as 86.8±2.6 km [*Baker and Stair Jr* (1988)]. Further, using OSIRIS data it has been shown that ground-based OH temperatures can be affected by changes in the OH emission layer height [*Sheese et al.* (2014)] which could lead to an uncertainty in tempera-

tures of the order of ±2–4 K (and up to ∼7 K in extreme cases as seen during 2009 major SSW event over high latitudes). However, as it can be seen from Figures 5.1c and 5.1d the enhancement in the NIRIS derived temperatures are much larger and therefore are believed to be due to SSW related effects and not by layer movement. This interpretation is confirmed by satellite-based measurements (as shown below in section 5.5).

5.4.2 MERRA Temperatures and Winds for 2004-2013

In Figure 5.2, the stratospheric temperature (T_S) in the polar cap region (poleward of 60^oN) and longitudinally averaged zonal wind (U_S) at 60^oN from MERRA are shown for the years 2004–2013 (from DOY 1 to 65). Six major warming events occurred during the years in 2004, 2006, 2008, 2009, 2010, and 2013 wherein the zonal mean zonal winds at 60^oN at 10 hPa pressure level reversed from eastward to westward. Five minor events were observed in the years 2008 (three events), and one each in 2011 and 2012, wherein the temperature in the polar cap region at 10 hPa pressure level increased by more than 25 K without any reversal of zonal mean zonal winds. In Figure 5.2 the duration of all these events are marked by vertical dashed lines. A list of the duration together with the peak temperature and the minimum zonal wind during these periods is given in Table 5.1.

5.5 Results and Discussion

A description on the data analyses used, results obtained, and discussion on the global effects that seem to be occurring in the stratospheric-mesospheric system, especially during SSW times, will be presented in the following sections.

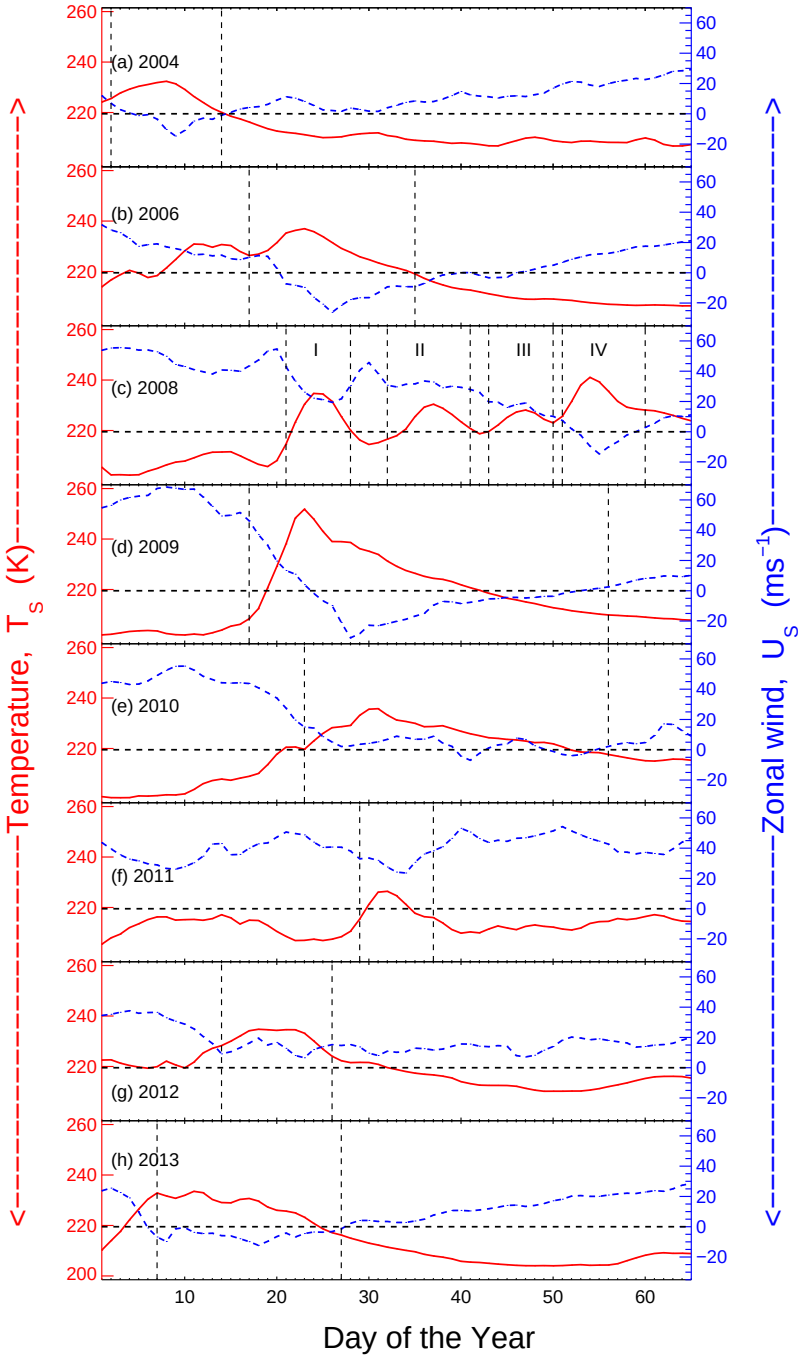

Figure 5.2: Temperatures in the polar cap poleward of 60^{o}N (T_S) and longitudinally averaged zonal wind at 60^{o}N (U_S) at 10 hPa pressure level (∼32 km) obtained from MERRA dataset for eleven SSW events which occurred during 2004–2013 that are selected for present study. The first 65 days of data for each of the eight years are shown. The duration of the SSW events are marked by vertical dashed lines.

Table 5.1: List of SSW events considered for this study

Year	DOY Range	T_{Smax}(K)	U_{Smin} (ms^{-1})
2004	2-14	232.37	-14.67
2006	17-35	236.96	-26.15
2008(I)	21-28	234.69	19.42
2008(II)	32-41	230.42	29.03
2008(III)	43-50	228.12	10.77
2008(IV)	51-60	241.06	-14.58
2009	17-56	251.83	-31.08
2010	23-56	235.77	-6.92
2011	29-37	226.41	23.61
2012	14-26	234.77	6.57
2013	7-27	233.53	-12.29

5.5.1 SABER, OSIRIS, and SOFIE Temperatures for 2009 and 2013 SSW Events

The latitudinal coverage of the TIMED satellite is 135^o, (83^o and 52^o in opposite hemispheres). Every 60 days the latitudinal coverage reverses due to periodic yaw manoeuvre of the satellite [*Russell III et al.* (1999)]. The latitudinal coverage of the SABER derived temperature data is approximately from 55^oS to 85^oN for the eleven SSW events considered in this study. Thus, the data are organized into a total of 15 ranges of 10^o latitude from 80^o–90^oN to 60^o–50^oS in the NH and SH. The SABER mean mesospheric temperatures (longitudinally averaged in the range of 2^o–142^o and in the altitude range of 85–89 km) are obtained at each of the 10^o latitudinal intervals for all the SSW events considered in this study.

Similarly, OSIRIS derived mean mesospheric temperatures (with similar longitudinal averaging as for the SABER data, but in the altitude range of 86–89 km) are obtained at each of the 10^o latitudinal intervals for all major SSW events. For all the given latitudinal ranges the daily mean mesospheric temperature from OSIRIS is derived wherever the number of data points is more than 10 for a given DOY.

The zonal mean mesospheric temperatures from SOFIE dataset are derived

with the latitude ranges poleward of 65^o in both hemispheres for all the major SSW events considered here.

In Figures 5.3a and 5.3b the blue coloured lines show SABER derived daily mean mesospheric temperature values at all the 15 latitude ranges as a function of DOY for the year 2013 and 2009, respectively, while the purple coloured lines show the SOFIE derived mean mesospheric temperatures over polar latitudes in both hemispheres. The dashed vertical lines in Figures 5.3a and 5.3b show the duration of the SSW events (DOY 7–27 in 2013 and DOY 17–56 in 2009). The dashed horizontal lines in Figures 5.3a and 5.3b show the mean mesospheric temperature (for a given latitude range) during the DOY ranges as indicated above for the 2013 and 2009 SSW events. From Figure 5.3a mesospheric cooling at high-latitudes ($>60^o$) over the NH is clearly seen during the SSW period especially during DOY 9–20 in both SABER and SOFIE data. As one moves from high- to low-latitudes the mesospheric cooling turn into mesospheric heating around mid-latitudes (during DOY 7–25 in 10^o–50^oN latitude range) before turning again to cooling over equatorial latitudes (during DOY 7–15).

The red coloured line in Figure 5.3a shows the NIRIS derived nocturnal mean OH temperatures obtained at Gurushikhar, Mount Abu, which is overlaid on the longitudinal mean mesospheric temperatures obtained from SABER datasets for the latitude range of 20^o–30^oN. From Figure 5.3a the NIRIS derived mesospheric temperatures are seen to be higher. This is not unexpected as the temperatures obtained by NIRIS are over a small FOV (zenith) and at a high data cadence as opposed to the SABER temperatures that are obtained by averaging a large longitude range (2^o–142^o). An enhancement in temperature is also noticed in the SH during DOY 10–23 (depending on the latitude).

In Figure 5.3b similar behaviour in the SABER and SOFIE derived mesospheric temperatures is seen for the major SSW events of 2009. The mesospheric cooling at higher latitudes ($>50^o$N) is clearly observed in both SABER

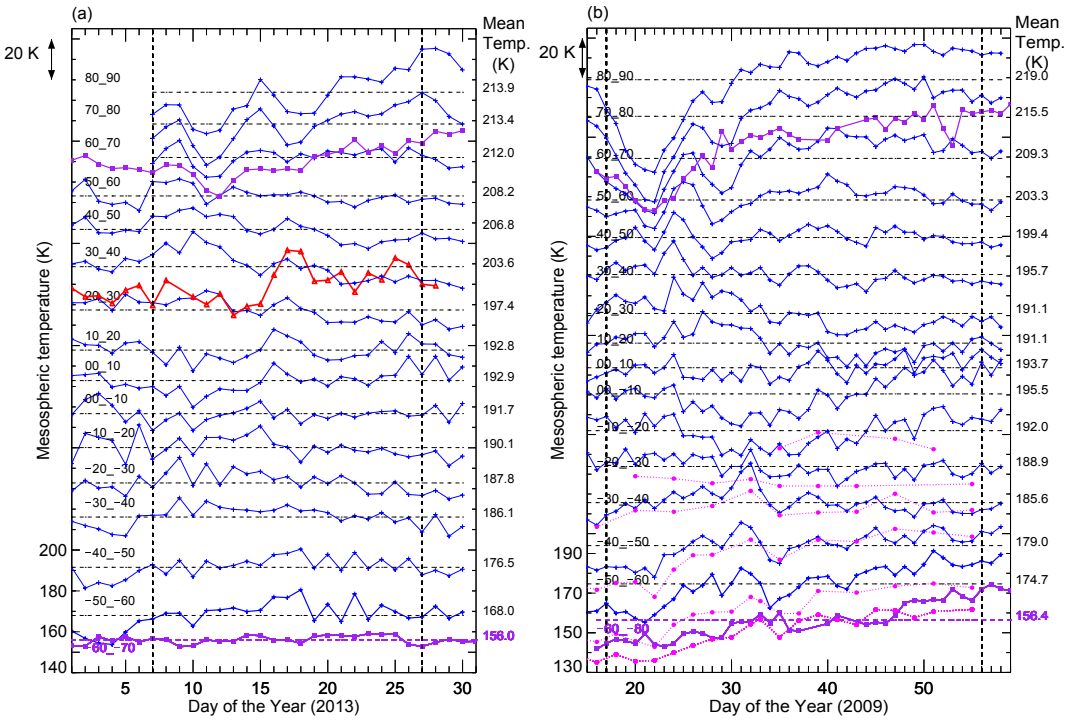

Figure 5.3: (a) Longitudinally (2^o-142^o) averaged mesospheric temperatures (averaged in the height range 85-89 km) derived from the SABER dataset at 10^o latitude interval (indicated in the top left of each sub panel) for both the hemispheres over 30 days (during DOY 1-30, 2013) are shown in blue coloured lines. NIRIS derived OH temperatures from Gurushikhar are overlaid in red colour. Vertical scale is for the bottom-most temperature variability, and the subsequent plots are shifted by 15 K. The horizontal dashed lines show the mean temperature values (for the DOY ranges indicated in the Table 5.1) which are shown on the right side. SOFIE derived zonal mean mesospheric temperatures at polar latitudes in NH and SH are shown by purple coloured lines. (b) Similar plot as shown in Figure 5.3a but for 2009 major SSW event in which in addition to SABER and SOFIE, OSIRIS derived mesospheric temperatures are also shown by magenta coloured lines at different latitudes.

and SOFIE derived mesospheric temperatures. The OSIRIS derived mesospheric temperatures are shown by magenta coloured lines in Figure 5.3b for the 2009 major SSW event since OSIRIS data are not available for 2013. For 2009 SSW event the OSIRIS temperatures are available in the SH from 10^o S to 90^oS for the altitude, latitude, and longitude ranges as discussed above. As can be seen from Figure 5.3b, the OSIRIS temperature trends for the given latitudinal range matches well with the SABER and SOFIE data with some differences in the absolute vales.

5.5.2 SABER Temperatures for 2006 and 2010 Major SSW Events

Similar to Figure 5.3 the latitudinal variations of mesospheric temperatures for 2006 and 2010 major SSW events are shown in Figures 5.4 and 5.5, respectively. As can be seen from both the Figures the mesospheric cooling at high-latitudes are quite evident for both major SSW events. The mesospheric warmings at mid-latitudes are also seen during both major SSW events.

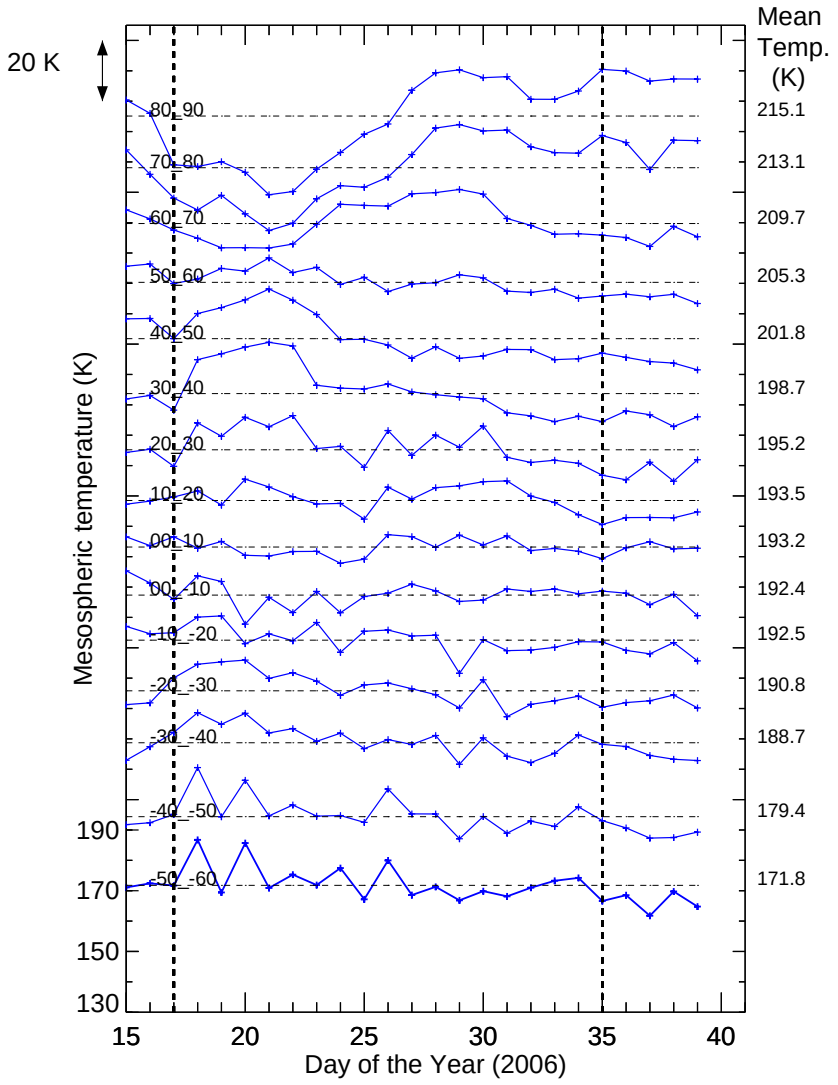

Figure 5.4: Similar to Figure 5.3 but for 2006 major SSW event.

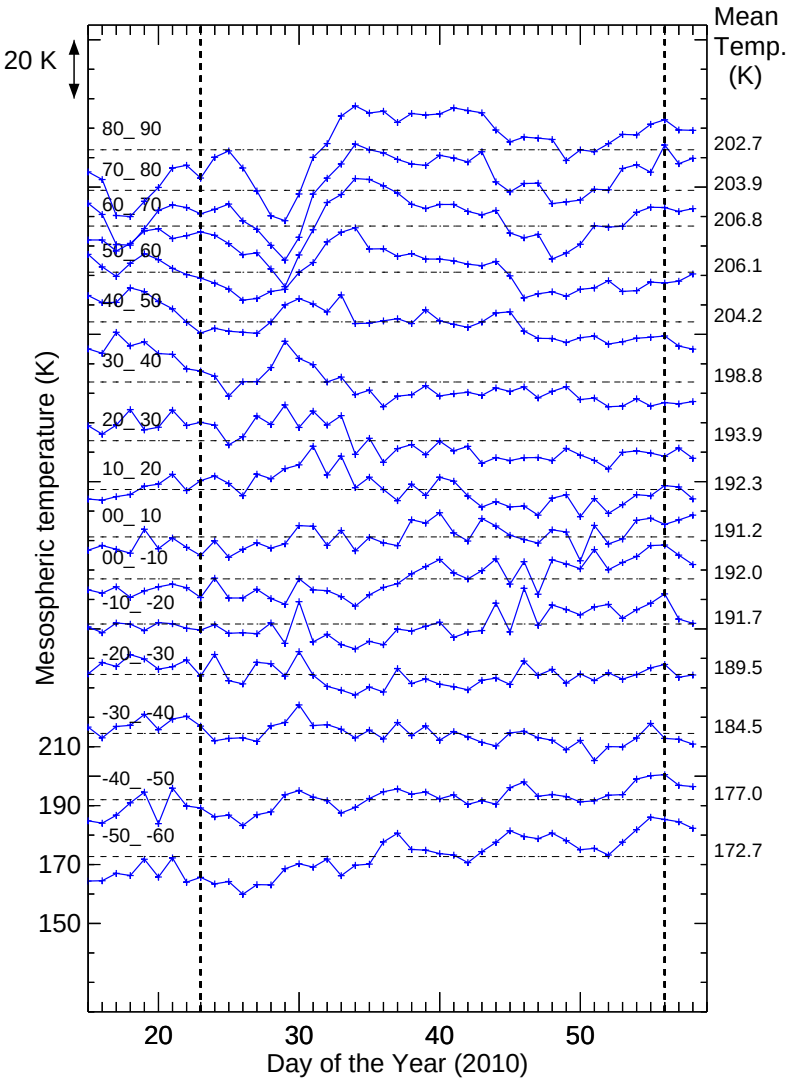

Figure 5.5: Similar to Figure 5.3 but for 2010 major SSW event.

5.5.3 SABER Temperatures for 2011 and 2012 Minor SSW Events

Similar to Figure 5.3 the latitudinal variations of mesospheric temperatures for two minor SSW events of 2011 and 2012 are shown in Figures 5.6 and 5.7, respectively. As can be seen form Figures 5.6 and 5.7 the mesospheric coolings at high-latitudes are not as evident as seen during the major SSW events.

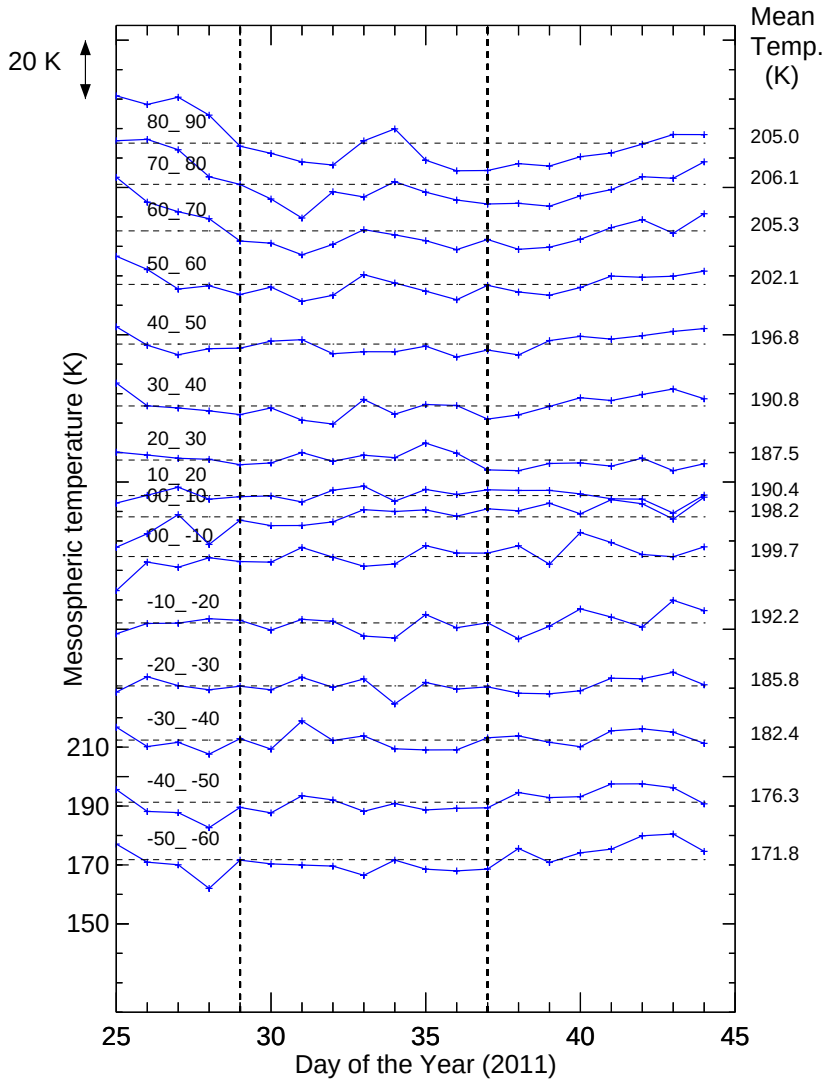

Figure 5.6: Similar to Figure 5.3 but for 2011 minor SSW event.

5.5.4 SABER Temperatures for 2008 SSW Events

Similar to Figure 5.3 the latitudinal variations of mesospheric temperatures for 2008 SSW event are shown in Figure 5.8. As can be seen from Figure 5.2, 2008 SSW event consists of three minor and one major SSW events. Since 2008 SSW event is a prolonged one mesospheric cooling at high-latitudes even during minor events of 2008(I) and 2008(II) can be seen clearly.

It may be noted that the transitions from cooling to warming from high- to low-latitudes in the NH and SH occur with some finite time delay indicat-

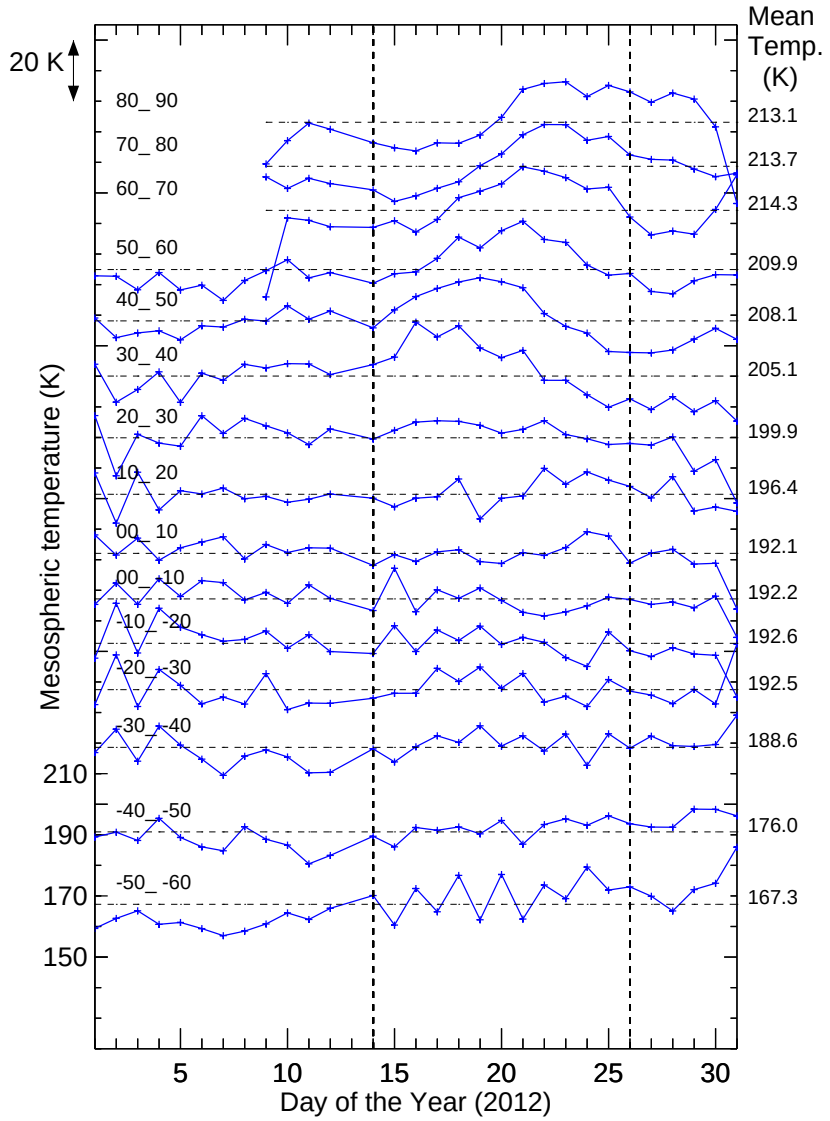

Figure 5.7: Similar to Figure 5.3 but for 2012 minor SSW event.

ing a physical transport of energy from high-latitudes in the NH to different latitudes extending to even those in the SH. Since the OSIRIS mesospheric temperatures are only available every other day and the data cadence for the SABER derived mesospheric temperatures are better. Therefore, further analysis has been carried out using SABER derived mesospheric temperatures. The observed latitudinal behaviour of the variability in the mesospheric temperatures has been characterized with respect to stratospheric temperatures poleward of 60^{o}N at 10 hPa pressure level during SSW events and is explained

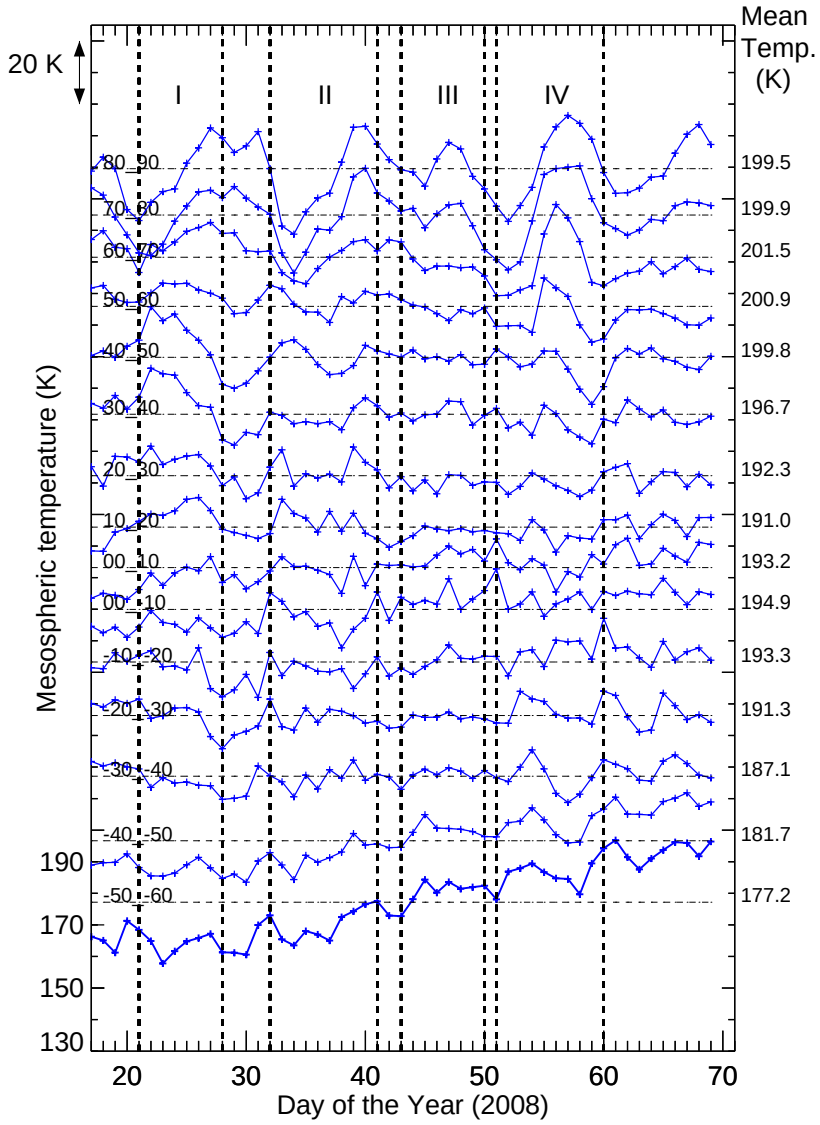

Figure 5.8: Similar to Figure 5.3 but for 2008 SSW event.

below.

5.5.5 Difference in Stratospheric vs Mesospheric Temperatures for 2009 and 2013 SSW Events

The mean mesospheric temperature for a given latitude range was obtained by averaging the temperature values over that latitude range for a week before and after the SSW period. The differences in mesospheric temperatures at

a given latitude range from the mean mesospheric temperatures (ΔT_M) are calculated for all the 15 latitude ranges for a given SSW duration. Similarly, the deviations in stratospheric temperatures (ΔT_S) from the mean value (calculated by averaging T_S over 60^o–90^oN for one week before and after the SSW event) are obtained using the MERRA dataset. As discussed earlier, there is a time delay in mesospheric response to the SSW events at high-latitudes that is different at different latitudes. Therefore, we have defined the post-SSW period as the one when the longitudinally averaged zonal wind at 60^oN at 10 hPa pressure level for the major SSW events becomes close to zero. The SSW periods are summarized in Table 5.1 and are also shown by vertical dashed lines in Figure 5.2 for all the eleven SSW events considered in this study.

As seen in Figures 5.3a and 5.3b the mesospheric temperatures at NH high-latitudes show cooling up to 60^o–70^oN during the SSW event with different behaviour at other latitudes. Correlation analyses have been performed between ΔT_S at high-latitude and ΔT_M obtained at different latitudes to investigate their interrelationships, if any. Figures 5.9a and 5.9b show the result of such analyses for some chosen latitude ranges for the 2013 and 2009 major SSW events, respectively.

In Figure 5.9, the horizontal and vertical axes represent stratospheric temperature deviation, ΔT_S, at high-latitude and mesospheric temperature difference, ΔT_M, at different latitudes as discussed above, and each "+" symbol represents a day during the SSW period. The slopes and the correlation coefficient for each of the latitude ranges are also shown in the respective panels. The high-latitudes (panels (i) and (ii) of Figures 5.9a and 5.9b) show a negative slope which indicates that increase in stratospheric temperatures, ΔT_S, is correlated with a decrease in mesospheric temperature, ΔT_M,which is consistent with general understanding. It is clearly seen (panels (iii)) that for 20^o–30^oN latitude range ΔT_M increases with increase in ΔT_S, indicating a mesospheric heating with respect to stratospheric warming. For the 0^o–10^oN latitude range ΔT_M decreases with increasing values of ΔT_S (panels (iv)). These observa-

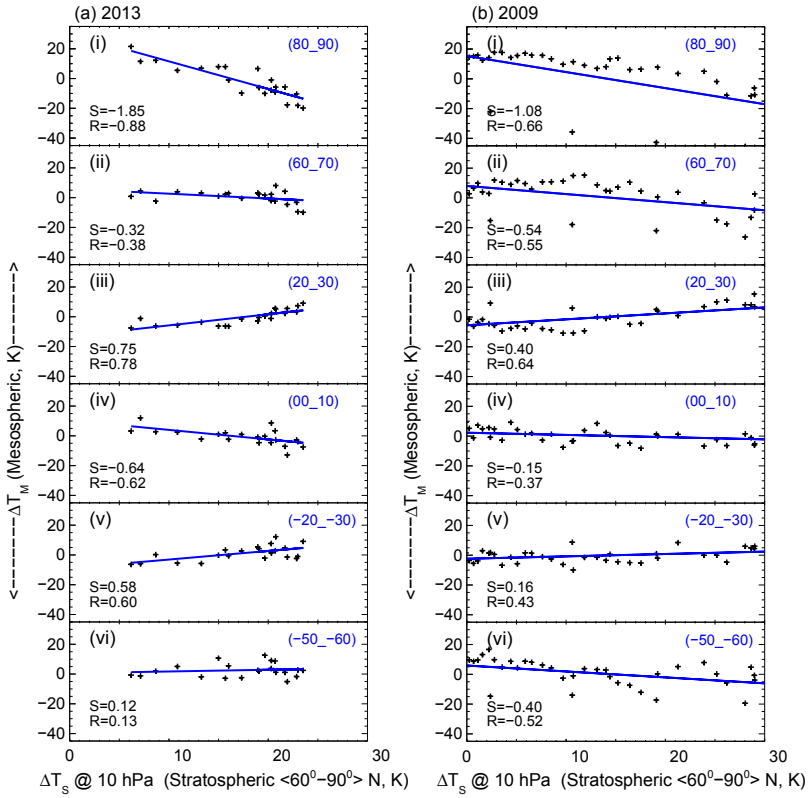

Figure 5.9: (a) Differences in SSW temperatures (ΔT_S) over 60^o–90^oN at 10 hPa pressure level vs difference in mesospheric temperatures (ΔT_M) for six selected latitude ranges for 2013 SSW event as derived from SABER datasets. (b) Similar plot as shown in Figure 5.9a but for 2009 SSW event.

tions show similar trends for all the major SSW events with different values of the slope for individual major SSW events. While the mesospheric cooling over high-latitudes during SSW has been reported in the literature, the excursions in the mesospheric temperatures over other latitudes as detailed here have not been reported before.

5.5.6 ΔT_S vs ΔT_M for Major and Minor SSW Events from SABER Data

The analyses relating the observed ΔT_M at different latitudes with ΔT_S at high-latitude as shown in Figure 5.9 for a few latitude ranges have been extended to all the 15 latitude ranges in Figure 5.10a. This Figure 5.10a includes

the three major SSW events of 2009, 2010, and 2013 as these were stronger and extended over a longer duration among the six major events considered in this study. Similarly, in Figure 5.10b the combined behaviour of ΔT_M with respect to ΔT_S for all five minor events at different latitude range is shown.

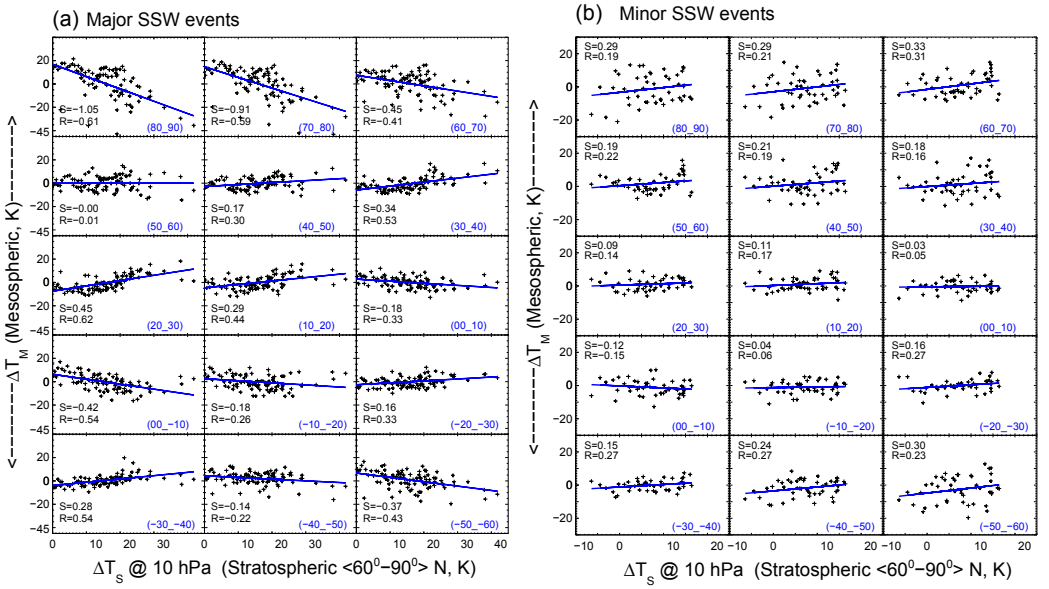

Figure 5.10: (a) Difference in SSW temperatures (ΔT_S) over 60^o–90^oN at 10 hPa pressure level vs difference in mesospheric temperatures (ΔT_M) at 10^o latitude intervals as derived from SABER dataset from both the hemispheres for three major SSW events of 2009, 2010, and 2013 for the durations as shown in Table 5.1. The latitudinal coverage to derive ΔT_M is shown in each plot in blue colour. The correlation coefficients (R) and the slopes (S) of the line are also shown in each sub-plot. A negative/positive slope with respect to an increase in ΔT_S indicates mesospheric cooling/warming at that latitude range. (b) Similar plot as shown in Figure 5.10a but for all five minor SSW events as shown in Figure 5.2. A better correlation is noted for major SSW events as compared to the minor ones.

Each "+" symbol in Figures 5.10a and 5.10b corresponds to a day during SSW period. From these scatterplots, correlation analyses have been performed and the slopes of the best fit lines obtained. The correlation coefficients (R) between ΔT_S and ΔT_M together with the slope of the best fit lines (S) are shown in each of the subplots in Figures 5.10a and 5.10b. It is apparent from the mesospheric temperature behaviour as shown in Figures 5.3 to 5.8 that the transitions in temperature from high- to low-latitudes occur during

different days (DOY's as discussed above) and is a non-linear phenomenon. Therefore, the linear fits shown in Figure 5.10 are a first order approximation of the variability between ΔT_S and $\Delta T_{M,}$ and hence, show smaller 'R' values than expected for a linearly varying phenomena.

Nevertheless, the slopes obtained by these linear fits do provide a broad 'visual' picture of the mesospheric temperature variability at different latitudes with respect to the stratospheric temperature changes at high-latitudes during SSW events. The slope (S) is positive if R is positive and vice-versa. Thus, the slopes of the best fit lines indicate the effect of the stratospheric temperatures enhancement (ΔT_S) on the mesospheric temperature differences (ΔT_M) at different latitudes. As mentioned above, a negative/positive slope indicates that there is a cooling/warming in the mesosphere in that latitude region. It is seen from Figure 5.10a that the slope is negative to begin with in the NH high-latitude (mesospheric cooling) and gradually turns positive (mesospheric heating) in mid- to tropical-latitudes. At latitudes closer to the equator we see a small negative slope, which, after crossing the equatorial-latitudes, turns positive before again turning negative over SH high-latitudes. The change of slopes from -1.05 at 85^oN farther away from equator as compared to -0.37 at 55^oS, indicates that the latitudinal temperature behaviour is asymmetric, with respect to the equator. For major events (Figure 5.10a) it is seen that in the NH, mesospheric cooling is seen up to 65^oN, and the peak in mesospheric heating occurs at 25^oN. In the SH, the mesospheric warmings peak at $\sim 35^oS$ and change to mesospheric cooling at $\sim 45^oS$. It may be noted that for major warming events (Figures 5.10a) there are stronger and systematic variations in the slopes as compared to the minor events (Figures 5.10b). For minor events the excursions of the slopes are in-and-around zero and the mesospheric cooling at the higher latitudes is not apparent. For both major and minor events, the SH mesospheric temperatures show smaller changes as compared to those in the NH.

5.5.7 ΔT_S vs ΔT_M for Major SSW events from SOFIE and OSIRIS Data

Using SOFIE data ΔT_M was calculated in a similar way as was done for SABER data discussed in the previous section. Figure 5.11a shows ΔT_S vs ΔT_M scatterplot using SOFIE data, which includes all three major SSW events of 2009, 2010, and 2013. As can be seen in this Figure the mesosphere in the 60^o–80^o latitude range for both NH and SH shows mesospheric cooling during major SSW events, which is in accordance with the trends observed using SABER data (Figure 5.10a for the NH). The data from SOFIE extends the coverage by 20^o latitude in the SH when compared with SABER.

As discussed earlier OSIRIS derived mesospheric temperatures are available from 20^o–85^oS. ΔT_M values have been calculated for every 10^o latitudinal intervals from 80^o–90^oS to 20^o–30^oS for 2009 and 2010 major SSW events and are shown in Figure 5.11b with respect to ΔT_S. The trends at different latitudinal coverage are similar to those estimated by SABER (Figure 5.10a). However, there are minor differences in the values of slopes which could be due to the fact that the OSIRIS data are available for alternate days and data for 2013 SSW event are not included in Figure 5.11b. Nevertheless, OSIRIS provides data polewards of 55^oS latitude which are not available from SABER and the values of slope show a somewhat constant behaviour polewards of 55^oS. This is in contrast to the steep slopes in the NH and is understood to be a consequence of SSW being a NH phenomenon.

It is important to note that independently obtained mesospheric temperatures from satellites do show an increase in mesospheric temperatures over tropical- to mid- latitudes during several major SSW events. These add credence to the ground-based NIRIS measurements that first indicated the existence of such a feature during the major SSW event of 2013.

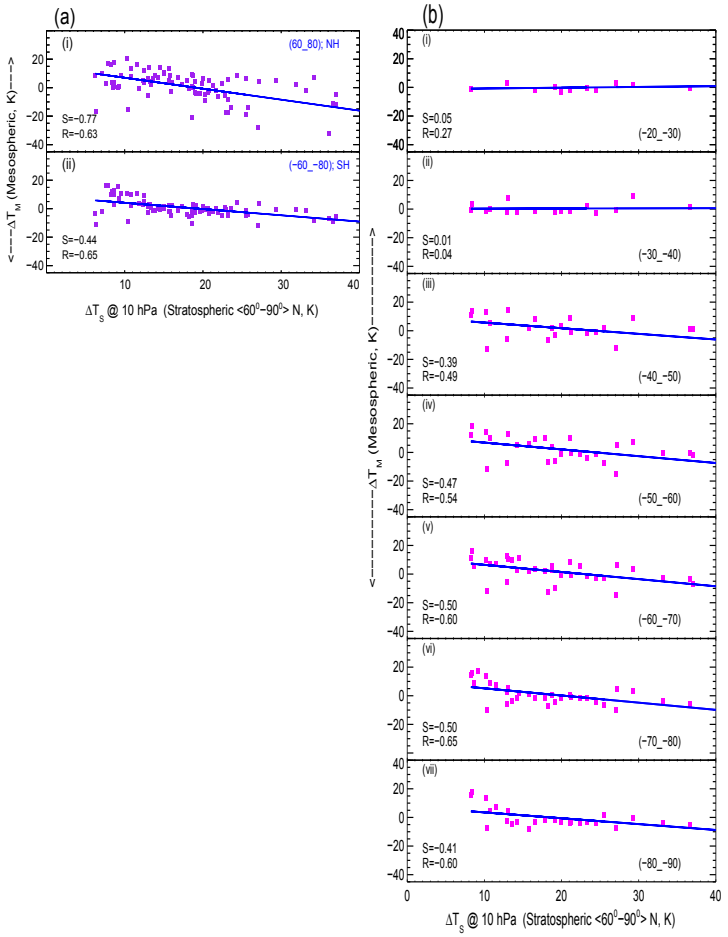

Figure 5.11: (a) Same as in Figure 5.9 but for SOFIE data at two latitudinal ranges in NH and SH for three major SSW events of 2009, 2010, and 2013 for the durations as shown in Table 5.1 combined together. The trends seen in this figure is in accordance with the one observed with the SABER data (Figure 5.10a). (b) Same as in Figure 5.9 but for OSIRIS data for two major SSW events of 2009 and 2010 for the durations as shown in Table 5.1. In spite of lower data cadence as seen in this figure compared to that as shown in Figure 5.10 from SABER data it is interesting to note that the trends are similar at different latitudinal ranges. As one move towards equator from SH polar latitudes the number of data points reduces. Also, OSIRIS data shows that the slopes remain constant poleward of 55°S during major SSW events.

5.5.8 Slope ($\Delta T_M/\Delta T_S$) vs Geographic Latitude for Major and Minor SSW Events

To investigate the characteristic behaviour of individual events, plots such as those shown in Figure 5.10, have been made for each of the eleven events

considered in this study (plots not shown here) and the variations in their slopes with respect to latitude are plotted in Figures 5.12a and 5.12b for major and minor events, respectively.

The geographic latitudes marked in Figure 5.12 are the midpoints of the 15 latitude ranges. The values of the slopes as obtained from Figures 5.10a and 5.10b are also shown as green coloured lines in Figures 5.12a and 5.12b respectively, to indicate the typical behaviour for major and minor SSW events. From Figure 5.12a it is clear that the NH polar mesosphere shows a cooling trend during major SSW events and this can even extend to 50^{o}N (as seen for the 2009 SSW event). However, as one moves equatorwards the mid-latitude mesospheric temperature shows warming effects. Closer to the equator, the mesospheric temperatures again indicate cooling. This trend is similar for all the major SSW events studied. Away from the equator towards mid-latitudes in the SH, the mesospheric temperatures again start increasing. A transition from mesospheric warming to mesospheric cooling is observed beyond the mid-latitudes in the SH as well, similar to the NH.

SABER measured mesospheric temperature data in the SH are available only up to 55^{o}S but, from OSIRIS data (Figure 5.6b) it can be seen that the mesospheric cooling further poleward of 55^{o}S is constant. The mesospheric warmings in the NH seem to be greater and distributed over a larger spatial extent when compared with the SH. This is seen in the characteristic "double-humped" structure in the slopes ($\Delta T_M/\Delta T_S$) with respect to the latitude during major SSW events. During minor SSW events (Figure 5.12b) no significant trend is noticed in the slopes derived for different geographic latitudes. During one of the minor SSW events of 2008 (marked as 2008_III in Figure 5.12b) the high-latitudes show warming, which turns to a cooling in the mid-latitude in NH, whereas, high-latitude over SH shows warmings. During the 2012 minor event the mid-latitude NH shows significant mesospheric warming. These two seem anomalous and at present, the reason for which is unknown.

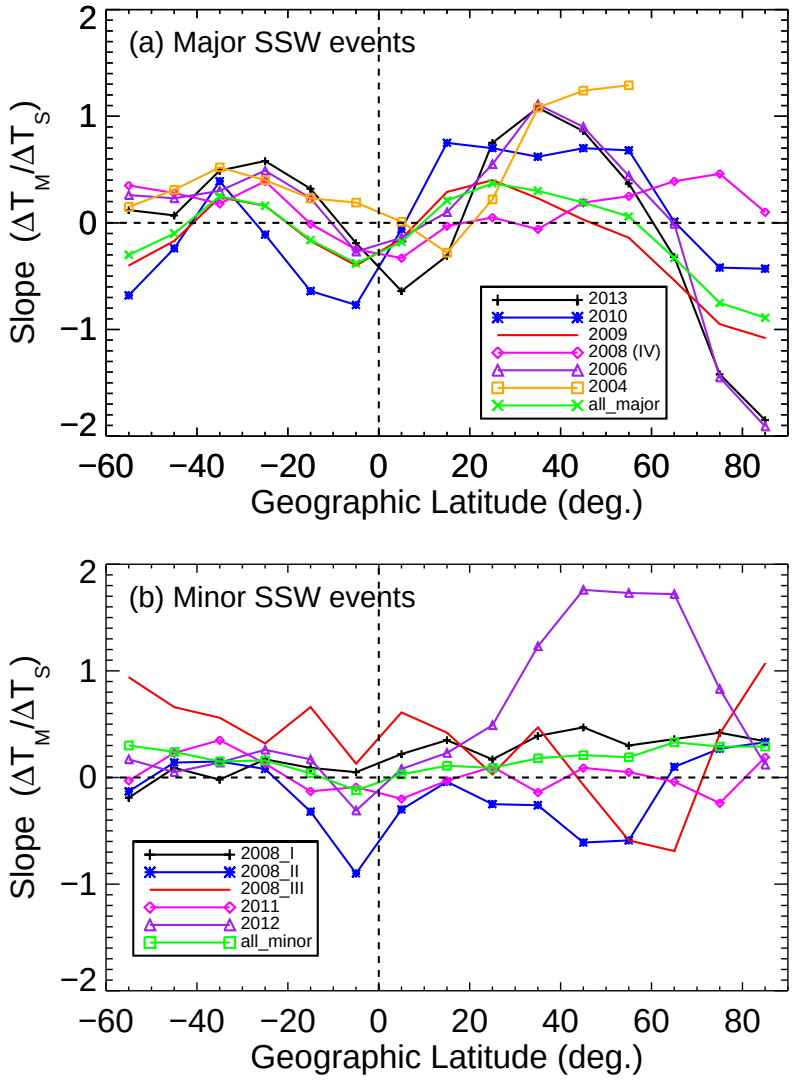

Figure 5.12: (a) Slopes ($\Delta T_M/\Delta T_S$) derived from analyses for each individual major SSW event using SABER data with respect to the geographic latitude (Figure 5.10 shows the slopes obtained for three major events combined together). Six major SSW events occurred during northern hemisphere winter months during 2004, 2006, 2008, 2009, 2010, and 2013. For the 2004 SSW period, the SABER derived mesospheric temperature data are available only up to 60^oN latitude. (b) Similar plots as in Figure 5.12a but for the minor SSW events, which occurred during northern hemisphere winter months for the three minor events of 2008, 2011, and 2012. The green curves in Figures 5.12a and 5.12b show the slope values as obtained from Figures 5.10a and 5.10b. One may note the "double-humped" structure in temperature ratios with respect to the geographic equator during major SSW events. For minor events, on an average, the slopes are in-and-around-zero.

5.5.9 Relationship between SRL with T_{Smax} and D with T_{Smax}

As can be seen from Figure 5.12, the variation in slopes at different latitudes for different SSW events are organized in a similar fashion. However, to investigate if there is any order in this behaviour with respect to the strength of SSW events, the latitudes of slope reversals from negative to positive values in both hemispheres as a function of peak stratospheric (at 10 hPa pressure level) temperature (T_{Smax}) poleward of 60^oN are shown in Figure 5.13a. The slope reversal latitudes (SRL) from positive to negative or vice-versa are very distinct during major SSW events (as shown in Figure 5.12a). However, slope reversals are not so evident during minor SSW events (Figure 5.12b). For the minor SSW events the latitudes of slope reversals are found by considering either the latitudes at which the slope is zero, or latitudes of trend reversals, if the slope does not cross the zero level. The result of correlation between the peak SSW temperatures (T_{Smax}) and the latitudes of slope reversals in both hemispheres in the poleward directions are plotted in Figure 5.13a.

Red/blue colour shows the best fit plots for NH/SH together with the R values. From Figure 5.13a we find a linear relationship (R=-0.66) between T_{Smax} and the SRL in the poleward side of NH. It indicates that when T_{Smax} is large, the mesospheric cooling over high-latitudes in the NH extends further towards mid-latitudes. From the same figure we find a linear relationship (R=-0.45) between T_{Smax} and the SRL in the poleward side of SH. The R values are better in the NH as compared to the SH, possibly due to the fact that the SSW events are NH phenomena. The relationship between SRL in term of SSW strengths, T_{Smax}, in the poleward direction in both NH and SH considering all the eleven SSW events (including major and minor) are given below:

$$SRL_{NH} = -1.3 \times T_{Smax} + 380.67 \tag{5.1}$$

$$SRL_{SH} = -0.44 \times T_{Smax} + 151.25 \tag{5.2}$$

where T_{Smax} and SRL are measured in K and degrees, respectively. Equatorward transition latitudes have not been considered as they are not structured as that of poleward transitions.

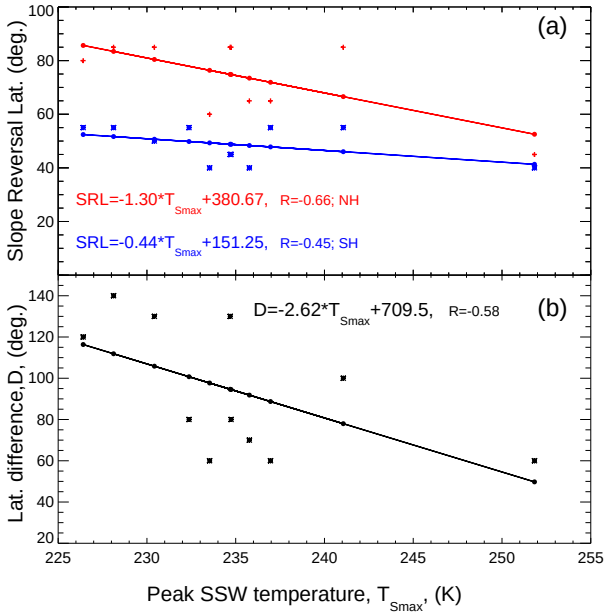

Figure 5.13: (a) Peak stratospheric temperature achieved over 60^o–90^oN latitude at 10 hPa pressure level for all the eleven selected SSW events are plotted with slope reversal latitudes in the poleward direction in both hemispheres. (b) Latitudinal difference in peak slopes of the "double-humped" structure as obtained from Figure 5.12 with respect to the peak stratospheric temperatures for all eleven SSW events are shown, which indicate an inverse relationship between them.

From Figure 5.12 it is seen that the latitudes of peak positive slopes in both the hemispheres are different for all the SSW events considered as the strengths of each event differs from the other. T_{Smax} during an SSW event and the difference, D, between the latitudes of peak positive slopes in the NH and SH (of the "double-humped structure") are plotted in Figure 5.13b for all the eleven SSW events. It is interesting to note that when T_{Smax} is greater, the latitudinal difference between NH and SH maxima in mesospheric warming at mid-latitudes decreases and vice versa. T_{Smax} and D are related linearly as:

$$D = -2.62 \times T_{Smax} + 709.5 \tag{5.3}$$

where T_{Smax} and D are measured in K and degrees, respectively.

Thus, through the characterization in this work, it can be appreciated that just by the knowledge of T_{Smax} (which is available in the public domain) a first order approximation on the behaviour of latitudinal mesospheric temperature structure can be made. From equations 5.1 and 5.2 the poleward transition latitudes of mesospheric temperature (from cooling to heating) can be obtained in both the hemispheres. From equation 5.3 the latitudinal difference, D, between the peak positive slopes can be obtained for any SSW event. It is known that the mesospheric temperature behaviour and its variation with respect to latitudes (and altitude) is a non-linear process. In all the characterizations attempted in this study, the behaviour of mesospheric temperature has been made considering only a linear approximation. Nevertheless, this empirical characterization is an attempt to obtain a broad picture of mesospheric temperature variation with respect to latitudes during SSW events.

5.5.10 SABER vs CIRA Temperatures Comparison During SSW Events

Figure 5.14a shows SABER derived mean mesospheric temperature during the periods shown in Table 5.1 for all the eleven SSW events as a function of geographic latitudes and are compared with the COSPAR International Reference Atmosphere (CIRA-86) model [*Fleming et al.* (1990)]. CIRA model outputs provide an estimation of temperature, zonal wind, and geopotential/geometric height as a function of altitude from 0–120 km altitudes in the latitudinal range of 80^oS to 80^oN.

The CIRA zonal mean temperatures have been averaged for the altitude range from 84.8 to 89.2 km and over 10^o latitudes for the months of January and February and are shown as the red dashed line in Figure 5.14a together

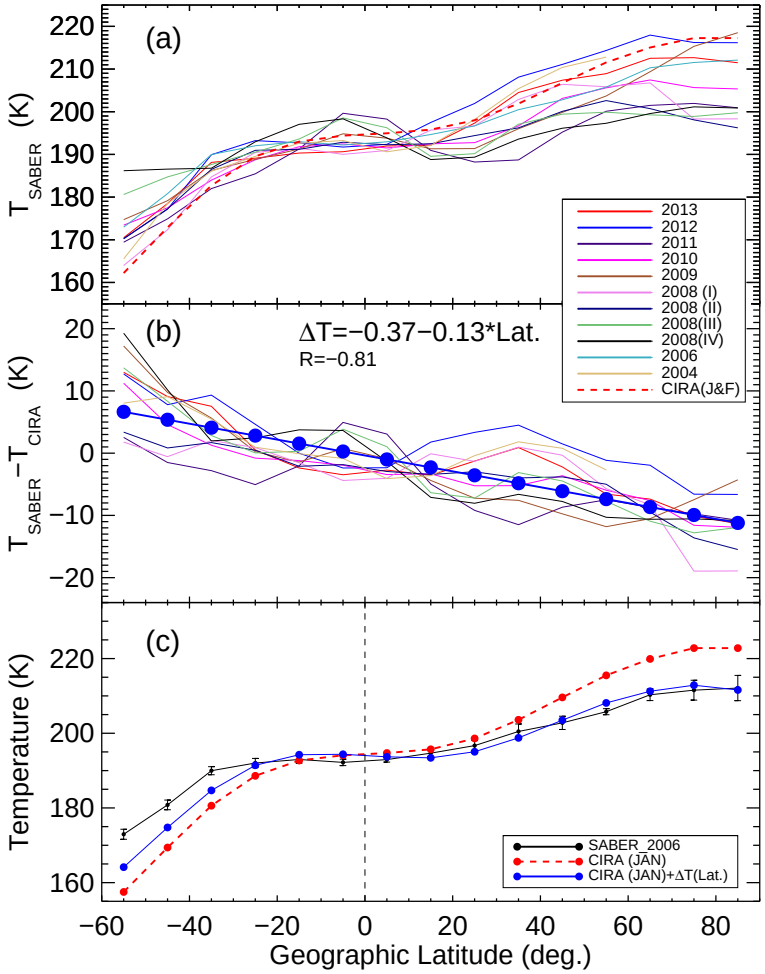

Figure 5.14: (a) Daily mean mesospheric temperatures derived from SABER data during SSW periods for all the eleven SSW events considered in this study with respect to geographic equator are shown. CIRA-86 derived temperature values averaged for the month of January and February are also shown in dashed red line. The CIRA-86 temperatures seem to overestimate/underestimate the values in the NH/SH. (b) The differences in the SABER measured and CIRA-86 estimated mesospheric temperature for the month in which the SSW event occurred (except for the 2006 event which is used for validation as shown in panel c) are shown. A linear relationship is also seen between T and geographic latitude. (c) SABER measured mesospheric temperatures (black) for the event of January 2006 (see Table 5.1) together with the standard error, CIRA-86 derived mesospheric temperatures (dashed red) for the month of January are shown. It may be noted that the CIRA estimated temperature values are higher/lower in the NH/SH high-latitude than the SABER measured value. The blue line shows the temperature values after accounting for the corrections as arrived at in equation 5.4 (shown in Figure 5.14b) in the CIRA derived values, which shows a better agreement with the SABER measured values.

with all the eleven SSW events that occurred during these two months. The temperature difference (ΔT) between the observed (SABER) and the modelled (CIRA-86) values for the months in which SSW events occurred have been obtained and are shown in Figure 5.14b as a function of geographic latitude. As seen from Figures 5.14a and 5.14b the CIRA-86 seems to overestimate the mesospheric temperatures in the NH and underestimate them in the SH, especially over high-latitudes. As it can be seen from Figure 5.14b, extreme ΔT values can be up to +20 K in the SH and -20 K in the NH showing a large range, which is due to the fact that different SSW events have different background conditions. A linear relationship has been obtained between the correction to be applied, ΔT (in K) and geographic latitudes (in degrees) as shown below:

$$\Delta T = -0.13 \times Lat - 0.37 \tag{5.4}$$

It should be mentioned here that in obtaining the equation 5.4 we have not considered the 2006 event as that event is used to validate this relationship. In Figure 5.14c the SABER derived mesospheric temperature values for the year 2006 are shown as a black curve together with the standard error. As it can be seen, the standard error is larger at NH polar latitudes showing large range of variations in mesospheric temperatures during SSW period. The red dashed curve shows the zonal mean mesospheric temperatures as obtained from CIRA model for the month of January (averaged for the altitude range from 84.8 to 89.2 km and over 10^o latitudes). To these CIRA values, the latitude dependent correction shown by equation 5.4 has been applied and the resulting values are shown by the blue coloured line. It can be seen that the correction shown by equation 5.4 brings the CIRA modelled mesospheric temperature values closer to the SABER measured values.

5.6 Summary and Conclusion

Ground-based spectroscopic measurement of mesospheric rotational temperatures from O_2 and OH bands originating at 94 km and 87 km altitudes as obtained from NIRIS from Gurushikhar (24.6^{o}N, 72.8^{o}E), a low-latitude location in India, showed enhanced temperatures (compared to their monthly mean values) during the SSW event of January 2013. This led to a wider investigation to understand mesospheric temperature changes over low-latitudes and to characterize the behaviour of mesospheric temperature variation as a function of geographic latitude during an SSW period with respect to the stratospheric (at 10 hPa pressure level) temperatures over high-latitude (60^o–90^{o}N). In this regard, SABER derived mesospheric temperatures for eleven SSW events which occurred during 2004–2013 have been considered. OSIRIS and SOFIE measured mesospheric temperatures are also considered, when available, and both showed broad similarity in their behaviour with SABER data. A detailed analyses of all of these independent measurements has revealed that there is a mesospheric heating over tropical- to mid- latitudes, more so in the NH, during major SSW events. All the major SSW events studied showed well-known mesospheric cooling over NH high-latitudes. Closer to the equatorial-latitudes the mesospheric heating turns into cooling and again turns to heating over mid-latitudes in the SH before turning to cooling over the SH high-latitude regions.

The "double-humped" structure in the mesospheric to stratospheric temperature ratios ($\Delta T_M/\Delta T_S$) vs latitude is very clear during major SSW events with two crests over tropical- to mid-latitudes and a trough over the geographic equator. Mesospheric temperatures during minor events do not show formation of such "double-humped" structure. A relationship between slope reversal latitudes (SRL) towards poleward side in terms of the peak SSW temperature, T_{Smax}, is obtained for both hemispheres [SRL_{NH} = -1.3 × T_{Smax} + 380.67 and SRL_{SH} = -0.44 × T_{Smax} + 151.25]. Further, it is found that the latitu-

dinal difference (D) between the two crests in the observed "double-humped" structure is related linearly with T_{Smax} as: D = -2.62 × T_{Smax} + 709.5.

It is also found that the CIRA-86 derived mesospheric temperatures overestimate the values in the NH and underestimate them in the SH as compared to the SABER measured temperatures, which is more prominent at the higher latitudes. A linear relationship has been obtained between the differences in SABER and CIRA derived mesospheric temperatures (ΔT) as a function of latitude ΔT= -0.13 × Lat - 0.37; wherein ten SSW events have been considered. Thus, with just the knowledge of the peak SSW temperatures, T_{Smax}, the mesospheric temperature behaviour with respect to latitude can be determined and their magnitudes with respect to latitudes can be found by applying the above mentioned correction to the CIRA model temperatures. Moreover, from the results presented in this study, a hitherto unknown aspect of the relationship between stratospheric temperature at high-latitude and mesospheric temperatures at different latitudes has been brought to light. These results strongly support the interactions in stratospheric-mesospheric coupling and high- to low-latitude coupling of mesosphere lower thermosphere region, especially during SSW events.